Planar chiral plasmonic 2D metamaterial: Design and Fabrication

Andrea Veroli[1,a)], Badrul Alam[2], Luca Maiolo[3], Francesco Todisco[4], Lorenzo Dominici[4], Milena De Giorgi[4], Giorgio Pettinari[5], Annamaria Gerardino[5] and Alessio Benedetti[1]

[1]*Department of Information Engineering, Electronics and Telecommunications, University of Rome La Sapienza, Via Eudossiana, 18, 00184 Rome, RM, Italy.*
[2]*Department of Electrical and Information Engineering, Polytechnic of Bari, Via Orabona, 4, Bari 70125, Italy.*
[3]*Istituto per la Microelettronica e Microsistemi - Consiglio Nazionale delle Ricerche, Via Fosso del Cavaliere 100, 00133, Roma, Italy.*
[4]*CNR NANOTEC, Istituto di Nanotecnologia, via Monteroni, 73100, Lecce, Italy.*
[5]*Institute for Photonics and Nanotechnologies, IFN-CNR, Via Cineto Romano 42, Rome, 00156, Italy.*

[a)]Corresponding author: andrea.veroli@uniroma1.it

Abstract. Metamaterials presenting a high circular dichroism are highly sought for various possible applications. Geometries in literature present the choice between complex elaborate geometries and shallow performances. In this work, we introduce a new planar geometry for a plasmonic metamaterial array featuring a high CD over a large bandwidth. We present the details on the related design methodology and fabrication procedures. During design step, shape variations around the perfect values have also been simulated and taken into account, and the performance are robust. The planar geometry helps not only to simplify the fabrication processes, which makes it more accessible for various applications, inexpensive and industrially feasible.

INTRODUCTION

In the last decades, studies on metamaterials became popular for their ability to feature properties that are rare or absent in nature; particularly interesting are the metamaterials designed for electromagnetic application, which may open new research frontiers [1, 2]. Surface Plasmons (SP) are a physical phenomenon, which is of great interest in the field of nano-technologies, as it enables strong field localization and sub-wavelength scale optical elements [3]. Such characteristics can be used to develop a variety of optical devices, such as multilayer optical integrated circuits [4], high gain antennas [5–8], nano-resonators [9], etc. SPs optical traits, together with the metamaterials properties, make them particularly useful in modern scientific area such chemical/biological sensing and near-field microscopy [10, 11].

Plasmonic structures can also enhance interaction with circularly polarized light, and some exhibit strong chiroptical effect [12]; in the recent years chiral plasmonic nanostructures have gained substantial interest [13]. These structures exhibit a high circular dichroism (CD) compared to common biomolecules [14]; but in a combination of both the plasmons may shift molecular chirality of many biomolecules from UV to visible and amplify the natural CD of molecules [15]. This phenomenon is called Super Chirality, and many ways to exploit it are being researched in order to produce a high sensitivity device which can detect the handedness of a given molecule [16].

A large number of dichroic metasurfaces has been developed in the last years [17]. To the great variety of geometries that have been demonstrated corresponds a big variety of fabrication techniques and approaches, both top-down and down-top; in general, in quantitative terms of CD factor, the top-down approach is more successful. Three dimensional (3D) nanophotonic structures [18, 19] are notably difficult to produce, as they require complex, time-consuming and/or elaborate procedures. Stacked planar (2D) geometries require precise alignment and a high number of lithographic and deposition steps [20, 21]. A few simple planar structures have been successful, as their intrinsic

NANOINNOVATION 2018
AIP Conf. Proc. 2145, 020015-1–020015-6; https://doi.org/10.1063/1.5123576
Published by AIP Publishing. 978-0-7354-1890-5/$30.00

chirality is usually low [12, 22]; some of those usually requires the use of extrinsic chirality [23] or nonlinearities [22]. Thus, geometries in literature present the choice between complex elaborate geometries and shallow performances; ideally it would be interesting to have planar structures featuring performances of 3D structures. Such 2D structures may be built by following single step lift-off, which is a procedure often used successfully with various types of metamaterials [2, 24].

In this work, we present, design and fabricate a new planar geometry in a plasmonic metamaterial array with a theoretical CD over 50 % over a bandwidth of 100 nm. During design step, shape variations around the perfect values have also been simulated and taken into account. The planar geometry helps not only to simplify the fabrication processes, which makes it more accessible, inexpensive and industrially feasible, but also to possible biological measurements, because of the regularity of the surface for the attachment of cells [25, 26].

In section I we will present the geometry, report the numerical simulations and draw the theoretical considerations. In section II we will present the fabrication processes of the array. In the last section, the conclusions are drawn.

THEORETICAL AND NUMERICAL ANALYSIS

For our study, we will represent the CD as given in [23] i.e. the difference between the transmittances of the two circular polarizations divided by their average value, further divided by 2 in order to have a [0, 1] range:

$$CD = \frac{T_R - T_L}{T_R + T_L} \tag{1}$$

The metamaterial was designed to operate at the optical frequencies, with the metal layer placed upon an ITO - Glass substrate, and the incident wave that impinging the device starting from the glass side and leaving from the metallic layer. To exploit the plasmonic phenomena for the metal layer we opted for the noble metals as gold and silver and the cell-based order size of hundreds of nanometers. The initial geometry we have chosen for the design of the cell-based unit of the metamaterial was the spiral, because of the intrinsic chirality expected by its shape. So, we tested the both logarithmic and Archimedean spirals; the samples modelling has been performed through an accurate design and post-analysis into a full 3D numerical environment by varying different geometric parameters. We used Lumerical FDTD Solutions to perform all the simulations taking advantage of its core engine based on a finite-difference time-domain (FDTD) algorithm, and Mathworks Matlab was used for the postprocessing step. We performed a multiple set of simulations in order to take into account both of the two opposite signs of circular polarization and the particular multilayered structure of the samples substrate.

This latter is standard and composed of a thick glass layer matched with another 700 nm thick ITO layer, according to the experimental electrical resistance of 13 W/cm^2, and further covered with an extremely thin 2 nm-thick ITO-EMA layer. The extremely thick glass layer and its imperfectly parallel bounds, together with the temporal coherence of the light source used for the experimental measurements, suggests the impossibility to have a coherent superposition of forward travelling waves and the consequence formation of a spectral beating on experimental measurements. For this reason, we calculated the air-glass reflectance and transmittance spectra, on one hand, and we simulated the illumination of the outer artificial material in the FDTD model setting an illumination panel into the glass layer twice for the circular polarizations, on the other. The overall transmittance has been simply calculated by multiplying the two distinct contributions. ITO and ITO-EMAs refractive indexes can be found in the literature [27].

The FDTD setup takes into account the complex structure of the artificial material with the relative 120° rotations of its single units and their alignment along the nodes of a triangular array. Since the FDTD box of Lumerical adopts a cartesian subdivision of space with parallelepiped-like voxels, we adopted a careful cut of the boxs borders in order to respect the effective periodicity of the projected samples. Consequently, periodic boundary conditions (PBC) were assigned to the faces of the FDTD box laying orthogonal to the x or y axis. In perfectly regular configurations, it is sufficient to include the sole region surrounded by the thick line as shown in Fig. 1 to consider the systems periodicity. Since usually constructed samples are subject to small natural inhomogeneities, sometimes we selected several basic square sections and added small random perturbations to the geometrical parameters of the single units of the metamaterial to perform a primary averaging procedure of the overall transmittance; in most of our simulations we put up 2 x 2 arrays of basic boxes. Indeed, numerical inspections proved that small deformations in the cross section of identical resonators generated weak resonances each time differently located in the observed spectrum, especially for wavelength ¡ 590 nm. Thus, we enhanced the reliability of our analysis by adding a random second-order contribution to the radial profile of the scatterers, with a maximum amplitude of ¡ 10 nm and low-pass filtered

oscillations; we included several basic boxes with several different resonators into the same FDTD box to make this mixing procedure effective, and a subsequent averaging process allowed to underline and extract the stable part of our numerical predictions together with the suppression or reduction of inconsistent localized random responses.

Efficient perfect matching layers (PML) were assigned to the extremal z-faces of the FDTD box to suppress undesired reflections. A common spatial resolution length for all the simulations has been set to 10 nm along x and y, with the resolution along z being 5 nm. A high-density over-meshing box was added around the ITO layer, lowering the z-step to a more precise value of 0.7 nm to better fit with the small scale of the ITO layer. The FDTD simulation time has been set to 300 fs for all the studied cases. Since we projected these samples to filter circular polarizations of light in the far field, in the post-processing stage we removed contributions related to other diffraction modes than the fundamental one. It should be pointed out that, thanks to the particular symmetry of the system, it should be sufficient to simulate the numerical structure with a single linearly polarized source field, and after the extraction of the output fundamental mode, adding the resulting vector field with its rotated copy affected by a further phase delay of +- 90 to get the final output for both the circular polarizations. To rise the accuracy of our numerical analysis, we decided to simulate the system under investigation performing two distinct simulations associated to relatively orthogonal linear polarizations.

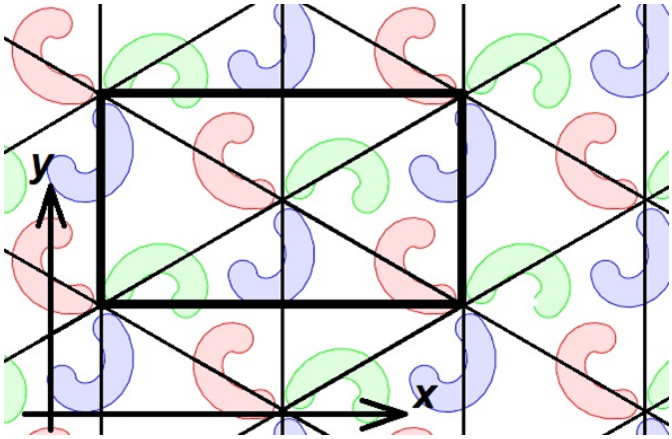

FIGURE 1. Schematic depiction of the system with the periodic alignment of units in a triangular array; the units are clones of the same unit rotated of 120° and collected into 3 different classes. The thick dark line highlights a sub-section which can be considered as the basic box to be included into the numerical space of Lumerical FDTD Solutions in order to respect the original periodicity.

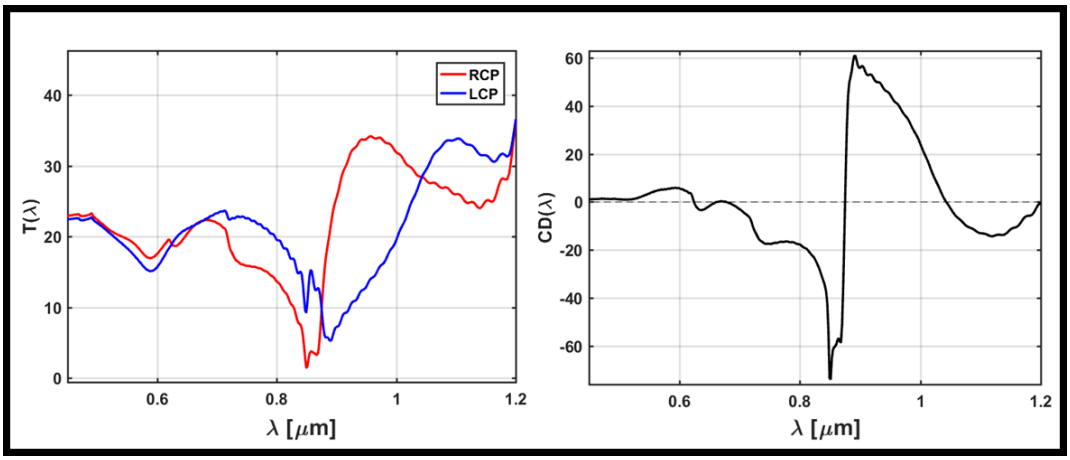

FIGURE 2. Numerical analysis results. On the left panel the transmission spectra: in red the right circular polarization (RCP) and in blue the left circular polarization (LCP); on the right panel the CD of the device. The metamaterial can reach a value over 50% of CD.

Numerical analyses were performed with the Archimedean spirals shape reduced to a fraction of its length i.e. its number of turns is around 0.35 and 0.5, and had a comma-like shape. The thickness was 180 nm. Three units are combined in "triplets", rotated from each other by 120°, and those are set within triangular supergrids (see Fig. 4). A shorter length means a lower single element occupation and thus a higher density of elements in the same area, which boosts the overall CD. In Fig. 2 are shown the numerical analysis results as function of transmission spectrums and CD Value, we can notice that the CD reach a giant value of 60 % in a bandwidth around of 100 nm (between 0.9 and 1.1 μm).

FABRICATION OF THE METAMATERIAL

We reported in Fig. 3 the scheme of the fabrication process flow, because the dimension of the metamaterial metal film is at nanometric scale, the key method for the fabrication is electron beam lithography (EBL), able to pattern nanometric structures. The process flow is the follow: a single layer of positive e-resist (PMMA AR-P series, 672.08, All-Resist) with a thickness of approximately 650 nm was spin-coated on the substrate, which is glass covered by a thin Titanium Indium Oxide layer (700 nm) on the top **(I)** (the standard procedure is described in [28]); then an EBL (Vistec EBPG 5HR) process is performed in order to pattern the structures **(II)**; the red and blue dotted lines schematize the different over-exposure effects from an area dose factor ***P*** to ***Pi***; after the development of the PMMA, **(III)** a Vacuum deposition of 5 nm Cr adhesion layer has been operated before deposition of the metal structural body (140 nm Au) **(IV)**; the lift-off was then completed with the removal of PMMA in acetone **(V)**.

The profiles of the realized elements depend strongly on the lithographic step, in particular on the exposure dose. In order to address the possible variations of the resulting structure, we patterned samples configuration in multiple areas by slightly tuning the electron beam dosage with the goal to find the optimum shape from the design. In Fig. 4 the fabrication results are shown.

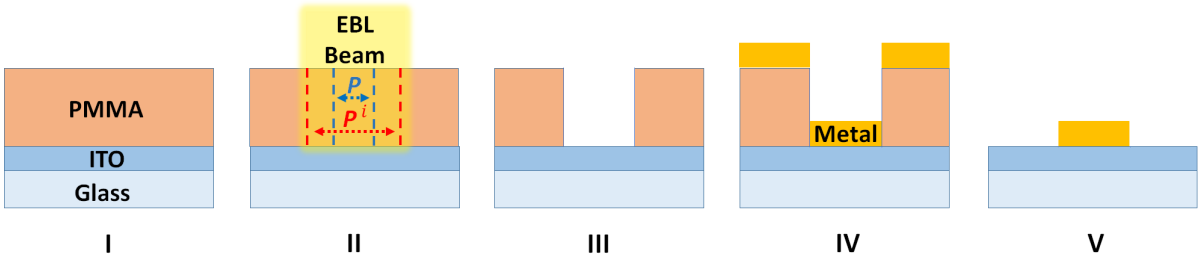

FIGURE 3. 2D Schematic fabrication process flow of the nano-commas.

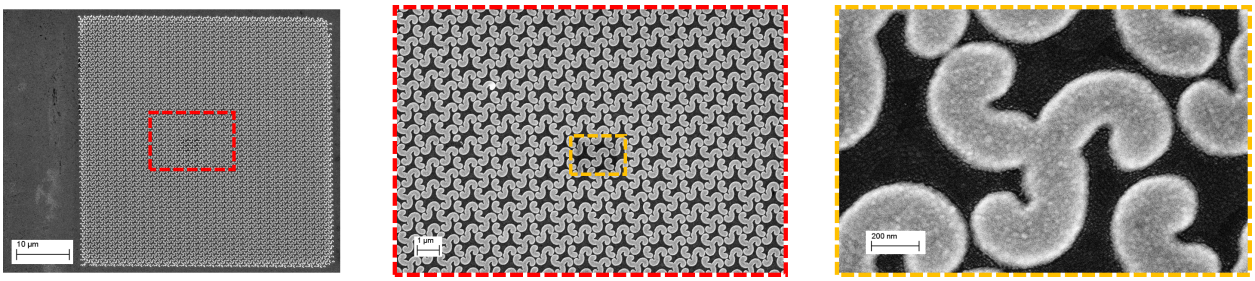

FIGURE 4. SEM images of the manufactured metamaterial. The figure reports a progressive zoom inspection of the device.

CONCLUSIONS

We have presented the design methodology and the fabrication procedures required to produce a highly dichroic metasurface based on a comma/bean-shaped geometry. We obtained high CD over a high bandwidth, performances comparable to metasurfaces requiring very elaborate and expensive fabrication methods. The structure can be fabricated through a single lithographic step by using liftoff process, as demonstrated by the realized samples. Moreover, our modelling method takes into account of the fabrication tolerances, and the performance is robust by design.

Overall, this work demonstrates the possibility to shift most of the complexity of the metamaterial development towards the design, in order to conversely simplify the fabrication and the characterization steps. This approach allows to produce more accessible devices for all the possible applications for dichroic metasurfaces.

ACKNOWLEDGMENTS

The authors wish to thank Dr. Francesco Mura and Prof. Caminiti for their support to the work.

REFERENCES

[1] N. I. Landy, S. Sajuyigbe, J. J. Mock, D. R. Smith, and W. J. Padilla, Physical review letters **100**, p. 207402 (2008).
[2] M. D. Astorino, R. Fastampa, F. Frezza, L. Maiolo, M. Marrani, M. Missori, M. Muzi, N. Tedeschi, and A. Veroli, Scientific reports **8**, p. 1985 (2018).
[3] S. A. Maier, *Plasmonics: fundamentals and applications* (Springer Science & Business Media, 2007).
[4] B. Alam, A. Veroli, and A. Benedetti, Journal of Applied Physics **120**, p. 083106 (2016).
[5] G. Calò, G. Bellanca, B. Alam, A. E. Kaplan, P. Bassi, and V. Petruzzelli, Optics express **26**, 30267–30277 (2018).
[6] G. Calò, G. Bellanca, A. E. Kaplan, P. Bassi, and V. Petruzzelli, Optical and Quantum Electronics **50**, p. 261 (2018).
[7] G. Bellanca, G. Calò, A. E. Kaplan, P. Bassi, and V. Petruzzelli, Optics express **25**, 16214–16227 (2017).
[8] M. Centini, A. Benedetti, M. Larciprete, A. Belardini, R. L. Voti, M. Bertolotti, and C. Sibilia, Physical Review B **92**, p. 205411 (2015).
[9] A. Benedetti, A. Belardini, A. Veroli, M. Centini, and C. Sibilia, Journal of Applied Physics **116**, p. 164312 (2014).
[10] O. S. Wolfbeis, Analytical chemistry **74**, 2663–2678 (2002).
[11] K. Kurihara, H. Ohkawa, Y. Iwasaki, O. Niwa, T. Tobita, and K. Suzuki, Analytica Chimica Acta **523**, 165–170 (2004).
[12] V. K. Valev, J. J. Baumberg, C. Sibilia, and T. Verbiest, Advanced Materials **25**, 2517–2534 (2013).
[13] A. O. Govorov, Z. Fan, P. Hernandez, J. M. Slocik, and R. R. Naik, Nano letters **10**, 1374–1382 (2010).
[14] A. Benedetti, B. Alam, M. Esposito, V. Tasco, G. Leahu, A. Belardini, R. L. Voti, A. Passaseo, and C. Sibilia, Scientific reports **7**, p. 5257 (2017).
[15] A. O. Govorov, The Journal of Physical Chemistry C **115**, 7914–7923 (2011).
[16] N. A. Abdulrahman, Z. Fan, T. Tonooka, S. M. Kelly, N. Gadegaard, E. Hendry, A. O. Govorov, and M. Kadodwala, Nano letters **12**, 977–983 (2012).
[17] Z. Wang, F. Cheng, T. Winsor, and Y. Liu, Nanotechnology **27**, p. 412001 (2016).
[18] M. Esposito, V. Tasco, F. Todisco, A. Benedetti, D. Sanvitto, and A. Passaseo, Advanced Optical Materials **2**, 154–161 (2014).
[19] M. Esposito, V. Tasco, F. Todisco, M. Cuscunà, A. Benedetti, D. Sanvitto, and A. Passaseo, Nature communications **6**, p. 6484 (2015).
[20] N. Liu, H. Liu, S. Zhu, and H. Giessen, Nature Photonics **3**, p. 157 (2009).
[21] C. Helgert, E. Pshenay-Severin, M. Falkner, C. Menzel, C. Rockstuhl, E.-B. Kley, A. Tunnermann, F. Lederer, and T. Pertsch, Nano letters **11**, 4400–4404 (2011).
[22] V. K. Valev, J. J. Baumberg, B. De Clercq, N. Braz, X. Zheng, E. Osley, S. Vandendriessche, M. Hojeij, C. Blejean, J. Mertens, *et al.*, Advanced Materials **26**, 4074–4081 (2014).
[23] E. Plum, X.-X. Liu, V. Fedotov, Y. Chen, D. Tsai, and N. Zheludev, Physical review letters **102**, p. 113902 (2009).

[24] M. D. Astorino, F. Frezza, and N. Tedeschi, Journal of ElEctromagnEtic WavEs and applications **31**, 727–739 (2017).
[25] A.-L. Morel, R.-M. Volmant, C. Méthivier, J.-M. Krafft, S. Boujday, and C.-M. Pradier, Colloids and Surfaces B: Biointerfaces **81**, 304–312 (2010).
[26] S. Unser, I. Bruzas, J. He, and L. Sagle, Sensors **15**, 15684–15716 (2015).
[27] T. A. Kőnig, P. A. Ledin, J. Kerszulis, M. A. Mahmoud, M. A. El-Sayed, J. R. Reynolds, and V. V. Tsukruk, ACS nano **8**, 6182–6192 (2014).
[28] A. Veroli, F. Mura, M. Balucani, and R. Caminiti, "Dose influence on the pmma e-resist for the development of high-aspect ratio and reproducible sub-micrometric structures by electron beam lithography," in *AIP Conference Proceedings*, Vol. 1749 (AIP Publishing, 2016) p. 020010.